On the numerical simulation of friction constrained motions

Roland Glowinski †, LieJune Shiau†, Ying Ming Kuo‡ and George Nasser §

Department of Mathematics, University of Houston, Houston, TX 77204, U.S.A.
†Department of Mathematics,University of Houston-Clear Lake, Houston, TX 77058, U.S.A.
‡NASA Johnson Space Center, Houston, TX 77058, U.S.A.
§George Nasser, Nasser Engineering, Houston, TX 77058, U.S.A.

Abstract. In a previous article (ref. [1]), the authors discussed the time-discretization of those relations modeling some elasto-dynamical systems with friction. The main goal of this article is to address similar problems using more sophisticated friction models and novel computational techniques. The new models give a better description of the system behavior when the velocities are close to zero. These investigations are motivated by the need for more accurate friction models in the software simulating the motion of mechanical systems, such as the remote manipulators of the Space Shuttle or of the International Space Station. The content can be summarized as follows: We discuss first several models of the constrained motion under consideration, including a rigorous formulation involving a kind of dynamical multiplier. Next, in order to treat friction, we introduce an implicit-explicit numerical scheme which is unconditionally stable, and easy to implement. Finally, the above scheme is coupled, via operator-splitting, to schemes classically used to solve differential equations from frictionless elasto-dynamics. The above schemes are validated through a series of numerical experiments.

† correspondence should be addressed to (shiau@cl.uh.edu)

1. Introduction: Synopsis

Motivated by the real time simulation of *elasto-dynamical systems* with *dry friction* we introduced in ref. [1], a family of numerical schemes taking advantage of the existence of a *friction multiplier*; multiplied by an appropriate matrix this multiplier provides the friction forces. Discrepancies between simulations and real life results lead engineers to refine their friction models in order to improve simulation quality, particularly at very low relative velocities, i.e. when friction forces dominate the dynamics of the system under consideration. The modeling of friction constrained motions will be discussed in Section 2, where the splitting of the resulting models will be also investigated. In Section 3, we will describe an implicit-explicit time-discretization scheme well-suited to the treatment of pure friction models. In Section 4, we shall take advantage of the splitting techniques discussed in Section 2 to couple the scheme of Section 3 with schemes classically used for the discretization of smooth elasto-dynamical models. The numerical results presented in Section 5 show good convergence properties for the displacement, velocity vectors, and the friction multiplier. In order to speed-up the computation of the friction multipliers, a penalty/Newton method is introduced in Section 6; The related numerical results show that this approach speeds up considerably the numerical solution of those pure friction problems resulting from time-splitting without affecting the overall accuracy.

The modeling and simulation of dry friction phenomena has motivated a quite large literature; the models considered in this article are relatively simple ones belonging to the "folklore" of mechanical engineering; however they apply to a number of practical situations and provide well-suited benchmark problem to test novel ideas such as the use of operator-splitting techniques which seems to be new in this context (albeit extensively used for the numerical solution of problems in fluid mechanics). The variational inequality approach used in this article has been applied to the solution of a variety of friction problems in, e.g., [3] and [18]. The solution of closely related friction problems by other techniques is discussed in, e.g. [7], [8], [9], [10] and [19].

2. Modeling of friction constrained motions: Splitting of the model

Some remote manipulator system simulators use *finite number of degree of freedom* models, like the one below to describe *friction constrained motions*:

$$\begin{cases} M\ddot{X} + AX + C(sgn(\dot{X}) - \gamma(\dot{X})) = f \quad \text{on } (0,T), \\ X(0) = X_0,\ \dot{X}(0) = V_0, \end{cases} \tag{1}$$

where in equation (1):

(i) X is a *displacement* (here $X(t) \in \mathbf{R}^d$),

(ii) the *mass matrix* M is symmetric and positive definite,

(iii) the *stiffness matrix* A is symmetric and positive semi-definite,

(iv) the *friction matrix* C is diagonal, i.e. $C = diag(c_1, \cdots, c_d)$, with $c_i \geq 0, \forall i = 1, \cdots, d$ and $\sum_{i=1}^{d} c_i > 0$,

(v) $sgn(V) = \{sgn(v_i)\}_{i=1}^{d}, \quad \forall \quad V = \{v_i\}_{i=1}^{d} \in \mathbf{R}^d$,

(vi) $\gamma(V) = \{\gamma_i(v_i)\}_{i=1}^{d}, \quad \forall \quad V = \{v_i\}_{i=1}^{d} \in \mathbf{R}^d$, γ_i being a *nondecreasing Lipschitz continuous* function vanishing at 0 and such that $\lim_{\xi \mapsto \pm\infty} \gamma_i(\xi) = \pm\beta_i$, with $0 < \beta_i < 1$,

(vii) f is an *external force* such that $f \in L^2_{loc}(0, T; \mathbf{R}^d), \quad T \in (0, +\infty]$,

(viii) X_0 and V_0 belong both to $\mathbf{R}^d$.

Remark 2.1: The case $\gamma = 0$ has been discussed in refs. [1] and [2]. Typical functions γ_i are provided (with $\epsilon_i > 0$) by

$$\gamma_i(\xi) = \frac{\beta_i \xi}{\sqrt{\epsilon_i^2 + \xi^2}} \tag{2}$$

and

$$\gamma_i(\xi) = \begin{cases} \beta_i \xi/\epsilon_i & \text{if } |\xi| \leq \epsilon_i, \\ \beta_i sgn(\xi) & \text{if } |\xi| \geq \epsilon_i. \end{cases} \tag{3}$$

Operator γ has been introduced to take into consideration the following well-known fact: When there is dry friction, the force necessary to put the system into motion, starting from rest, is higher than the one necessary to maintain the motion. For "simplicity", we shall assume from now on that $c_i > 0, \forall i = 1, \cdots, d$.

The function $sgn\frac{\dot{X}}{|\dot{X}|}$ makes sense at those values of t where $\dot{X}(t) \neq 0$; On the other hand, it makes no sense for t such that $\dot{X}(t) = 0$. Actually, mechanical considerations (see, e.g., [3] and [19] for details, concerning the solution of related contact problems) lead to substitute to (1) the following system

$$\begin{cases} M\ddot{X} + AX + C\lambda - C\gamma(\dot{X}) = f & \text{on } (0, T), \\ C\lambda(t) \cdot \dot{X}(t) = \sum_{i=1}^{d} c_i |\dot{x}_i(t)|, \ \lambda(t) \in \Lambda \quad \text{a.e. on } (0, T), \\ X(0) = X_0, \ \dot{X}(0) = V_0, \end{cases} \tag{4}$$

where in (4), $a \cdot b = \sum_{i=1}^{d} a_i b_i, \forall a = \{a_i\}_{i=1}^{d}, b = \{b_i\}_{i=1}^{d} \in \mathbf{R}^d, \Lambda = \{\mu | \mu \in \mathbf{R}^d, |\mu_i| \leq 1, \forall i = 1, \cdots, d\}$, and $\dot{X} = \{\dot{x}_i\}_{i=1}^{d}$. It is clear that the first equation in (4) coincides with the corresponding one in (1) for those t such that $\dot{X}(t) \neq 0$, but still makes sense if $\dot{X}(t) = 0$.

In (4), the *multiplier* λ and the vector $\gamma(\dot{X})$ model the friction forces (via $C(\lambda - \gamma(\dot{X}))$). Proving the existence of a pair $\{X, \lambda\}$ verifying (4) is easy; inspired by ref. [3] (see also ref. [2]), we approximate (4) (and equation (1)) by

$$\begin{cases} M\ddot{X}_\eta + AX_\eta + C(\lambda_\eta - \gamma(\dot{X}_\eta)) = f \quad \text{on } (0, T), \\ X_\eta(0) = X_0, \dot{X}_\eta(0) = V_0, \end{cases} \tag{5}$$

with $\eta > 0$, and $\lambda_\eta = \{\dot{x}_{i\eta}/\sqrt{\eta^2 + \dot{x}_{i\eta}^2}\}_{i=1}^{d}$. Suppose that $0 < T < +\infty$ and $f \in L^\infty(0, T; \mathbf{R}^d)$; problem (5) has clearly a unique solution and, using *Ascoli's theorem*,

we can prove that

$$\lim_{\eta\to 0}\{X_\eta,\lambda_\eta\}=\{X,\lambda\}\text{ in }W^{2,\infty}(0,T;\mathbf{R}^d)\times L^\infty(0,T;\mathbf{R}^d)\text{ weak}-*, \tag{6}$$

where $\{X,\lambda\}$ is a solution (necessarily unique) of problem (4). Relation (6) implies that $\lim_{\eta\to 0}X_\eta = X$ in $C^1([0,T];\mathbf{R}^d)$. In order to *decouple* the numerical treatment of the *elasticity* and *friction* terms (AX and $C(sgn(\dot{X})-\gamma(\dot{X}))$, respectively, here), we observe that systems (1) and (4) are *equivalent* to

$$\begin{cases} M\dot{V}+C(sgn(V)-\gamma(V))+AX=f & \text{on } (0,T),\\ \dot{X}=V & \text{on } (0,T),\\ X(0)=X_0,\ V(0)=V_0, \end{cases} \tag{7}$$

and

$$\begin{cases} M\dot{V}+C\lambda-C\gamma(V)+AX=f & \text{on } (0,T),\\ \dot{X}=V & \text{on } (0,T),\\ C\lambda(t)\cdot V(t)=\sum_{i=1}^d c_i|v_i(t)|, & \lambda(t)\in\Lambda \text{ a.e. on } (0,T),\\ X(0)=X_0,\ V(0)=V_0, \end{cases} \tag{8}$$

respectively. Let N be a positive integer and $\Delta t = T/N$; we denote $n\Delta t$ by t^n. Among the many possible *operator-splitting schemes* "available" to time-discretize (7) and (8), we advocate the one below, particularly easy to implement (we consider the discretization of (8) only, (8) being more rigorous than (7)):

$$X^0=X_0,\quad V^0=V_0; \tag{9}$$

for $n=1,\cdots,N$, X^n and V^n being known, solve

$$\begin{cases} M\dot{V}+C(\lambda-\gamma(V))=f & \text{on } (t^n,t^{n+1}),\\ C\lambda(t)\cdot V(t)=\sum_{i=1}^d c_i|v_i(t)|, & \lambda(t)\in\Lambda \text{ a.e. on } (t^n,t^{n+1}),\\ \dot{X}=0 & \text{on } (t^n,t^{n+1}),\\ V(t^n)=V^n,\quad X(t^n)=X^n, \end{cases} \tag{10}$$

and set

$$V^{n+1/2}=V(t^{n+1}),\quad X^{n+1/2}=X^n, \tag{11}$$

solve

$$\begin{cases} M\dot{V}+AX=0 & \text{on } (t^n,t^{n+1}),\\ \dot{X}=V & \text{on } (t^n,t^{n+1}),\\ V(t^n)=V^{n+1/2},\quad X(t^n)=X^{n+1/2}, \end{cases} \tag{12}$$

and set

$$V^{n+1}=V(t^{n+1}),\quad X^{n+1}=X(t^{n+1}). \tag{13}$$

System (12) is *equivalent* to

$$\begin{cases} M\ddot{X}+AX=0 & \text{on } (t^n,t^{n+1}),\\ X(t^n)=X^{n+1/2},\quad \dot{X}(t^n)=V^{n+1/2}, \end{cases} \tag{14}$$

and

$$X^{n+1} = X(t^{n+1}), \quad V^{n+1} = \dot{X}(t^{n+1}). \tag{15}$$

The numerical solution of the sub-initial value problems (10) and (12), (14) will be discussed in Sections 3 and 4, respectively.

Remark 2.2:A symmetrized (in the sense of G. Strang [4]) variant of scheme (9)− (13) reads as follows (with $t^{n+1/2} = (n + 1/2)\Delta t$):

$$X^0 = X_0, \quad V^0 = V_0; \tag{16}$$

for $n = 1, \cdots, N$, X^n and V^n being known, solve

$$\begin{cases} M\dot{V} + C(\lambda - \gamma(V)) = f & \text{on } (t^n, t^{n+1/2}), \\ C\lambda(t) \cdot V(t) = \sum_{i=1}^{d} c_i |v_i(t)|, & \lambda(t) \in \Lambda \text{ a.e. on } (t^n, t^{n+1/2}), \\ \dot{X} = 0 & \text{on } (t^n, t^{n+1/2}), \\ V(t^n) = V^n, \quad X(t^n) = X^n, \end{cases} \tag{17}$$

$$V^{n+1/2} = V(t^{n+1/2}), \quad X^{n+1/2} = X^n, \tag{18}$$

$$\begin{cases} M\dot{V} + AX = 0 & \text{on } (0, \Delta t), \\ \dot{X} = V & \text{on } (0, \Delta t), \\ V(0) = V^{n+1/2}, \quad X(0) = X^{n+1/2}, \end{cases} \tag{19}$$

$$\hat{V}^{n+1/2} = V(\Delta t), \quad \hat{X}^{n+1/2} = X(\Delta t), \tag{20}$$

$$\begin{cases} M\dot{V} + C(\lambda - \gamma(V)) = f & \text{on } (t^{n+1/2}, t^{n+1}), \\ C\lambda(t) \cdot V(t) = \sum_{i=1}^{d} c_i |v_i(t)|, & \lambda(t) \in \Lambda \text{ a.e. on } (t^{n+1/2}, t^{n+1}), \\ \dot{X} = 0 & \text{on } (t^{n+1/2}, t^{n+1}), \\ V(t^{n+1/2}) = \hat{V}^{n+1/2}, \quad X(t^{n+1/2}) = \hat{X}^{n+1/2}, \end{cases} \tag{21}$$

$$V^{n+1} = V(t^{n+1}), \quad X^{n+1} = \hat{X}^{n+1/2}. \tag{22}$$

Remark 2.3: An interesting discussion, and comparisons of various *kinetic friction models*, can be found in [9, 10]. We definitely think that the computational methods discussed in the present article can be generalized to the treatment of some of the models discussed in the above references.

Remark 2.4: The following model (with $g > 0$)

$$\begin{cases} \frac{1}{c^2}\frac{\partial^2 u}{\partial t^2} - \frac{\partial^2 u}{\partial x^2} + g\lambda = 0 & \text{in } (0, L) \times (0, T), \\ \lambda \frac{\partial u}{\partial t} = |\frac{\partial u}{\partial t}|, \ |\lambda| \leq 1 & \text{in } (0, L) \times (0, T), \\ u(0, t) = u(L, t) = 0 & \text{in } (0, T), \\ u(x, 0) = u_0(x), \ \frac{\partial u}{\partial t}(x, 0) = u_1(x), \end{cases} \tag{23}$$

describes the friction constrained planar motion of an elastic string. This nonlinear wave model has been thoroughly analyzed in [7], [8], while its numerical simulation and boundary control have been discussed in [2] and [6]. After appropriate finite difference or finite element discretizations (23) leads to problems such as (1), with $\gamma = 0$.

3. Numerical solution of type (10) subproblems

3.1. Time-discretization of system (10)

Problem (10) is a special case of

$$\begin{cases} M\dot{W} + C(\lambda - \gamma(W)) = f & \text{on } (t_0, t_f), \\ C\lambda(t) \cdot W(t) = \sum_{i=1}^{d} c_i |w_i(t)|, & \lambda(t) \in \Lambda \text{ a.e. on } (t_0, t_f), \\ W(t_0) = W_0. \end{cases} \tag{24}$$

Suppose that $f \in L^\infty(t_0, t_f; \mathbf{R}^d)$; then problem (24) has a unique solution in $W^{1,\infty}(t_0, t_f; \mathbf{R}^d) \times L^\infty(t_0, t_f; \mathbf{R}^d)$. Let P be a positive integer and denote $(t_f - t_0)/P$ by τ_1. In order to time-discretize (24), we advocate the following implicit-explicit scheme:

$$W^0 = W_0; \tag{25}$$

for $p = 1, \cdots, P, W^{p-1}$ being known solve

$$\begin{cases} M\frac{W^p - W^{p-1}}{\tau_1} + C\ \lambda^p = C\gamma(W^{p-1}) + f^p, \\ C\ \lambda^p \cdot W^p = \sum_{i=1}^{d} c_i |w_i^p|, \qquad \lambda^p \in \Lambda, \end{cases} \tag{26}$$

where $f^p = f(t_0 + p\tau_1)$ (or an approximation of it). Concerning the solvability of problem (26), we have the following:

Theorem 3.1 *Problem (26) has a unique solution* $\{W^p, \lambda^p\}$.

Proof: Denote by b^p the vector $MW^{p-1} + \tau_1 C\gamma(W^{p-1}) + \tau_1 f^p$; problem (26) takes then the following form:

$$\begin{cases} MW^p + \tau_1 C\ \lambda^p = b^p, \\ C\ \lambda^p \cdot W^p = \sum_{i=1}^{d} c_i |w_i^p|, \quad \lambda^p \in \Lambda. \end{cases} \tag{27}$$

Define $j : \mathbf{R}^d \mapsto \mathbf{R}$ by

$$j(V) = \sum_{i=1}^{d} c_i |v_i|, \quad \forall V = \{v_i\}_{i=1}^d \in \mathbf{R}^d; \tag{28}$$

since $c_i > 0, \forall i$, functional $j(\cdot)$ is convex over $\mathbf{R}^d$. Next, take the scalar product with $(V - W^P)$ of both sides of the first equation in (27). We have then

$$MW^p \cdot (V - W^p) + \tau_1 (C\lambda^p \cdot V - C\lambda^p \cdot W^p) = b^p \cdot (V - W^p),\ \forall V \in \mathbf{R}^d. \tag{29}$$

Observing that

$$C\lambda^p \cdot W^p = j(W^p), \tag{30}$$

and (from $\lambda^p \in \Lambda$)

$$C\lambda^p \cdot V = \sum_{i=1}^{d} c_i \lambda_i^p v_i \leq \sum_{i=1}^{d} c_i |v_i| = j(V), \forall V \in \mathbf{R}^d, \tag{31}$$

it follows from (29)-(31) that

$$\left\{ \begin{array}{l} W^p \in \mathbf{R}^d, \\ MW^p \cdot (V - W^p) + \tau_1(j(V) - j(W^p)) \geq b^p \cdot (V - W^p), \forall V \in \mathbf{R}^d. \end{array} \right. \tag{32}$$

Observing that $M = M^t$, it follows from, e.g. [5] and [11] that (32) characterizes W^p as the solution of the *minimization problem*

$$\left\{ \begin{array}{l} W^p \in \mathbf{R}^d, \\ J(W^p) \leq J(V), \quad \forall V \in \mathbf{R}^d, \end{array} \right. \tag{33}$$

where $J : \mathbf{R}^d \mapsto \mathbf{R}$ is defined by

$$J(V) = \frac{1}{2} MV \cdot V + \tau_1 j(V) - b^p \cdot V, \quad \forall V \in \mathbf{R}^d. \tag{34}$$

By convexity argument (see again [5], [11]), we can show that M positive definite implies that problem (33) has a unique solution characterized by the existence of $\lambda^p \in \Lambda$, so that relation (27) holds. The uniqueness of W^p and the existence of C^{-1} implies the uniqueness of λ^p.

If $f \in C^0([t_0, t_f]; \mathbf{R}^d)$, we can easily show that $\forall \tau_1 (i.e., \forall P)$ we have

$$\left\{ \begin{array}{l} \|W^p\|_{\mathbf{R}^d} \leq \|W^0\|_{\mathbf{R}^d} + \|M^{-1}\|(2\sqrt{d}\|C\| + \|f\|_\infty)(t_f - t_0) \\ \forall p = 1, \cdots, P, \end{array} \right. \tag{35}$$

namely, the *unconditional stability* of scheme (25) - (26). Using, once more, *compactness* arguments, we can show that

$$\lim_{\tau_1 \to 0} max_{1 \leq p \leq P} \|W^p - W(t_0 + p\tau_1)\|_{\mathbf{R}^d} = 0. \tag{36}$$

Remark 3.1: Define λ_{τ_1} by $\lambda_{\tau_1} = \sum_{p=1}^{P} \lambda^p \chi_p$ where χ_p is the characteristic function of $(t_0, t_f) \cap (t_0 + \tau_1(p - 1/2), t_0 + \tau_1(p + 1/2))$. We have then $\lambda_{\tau_1} \in \tilde{\Lambda} = \{\mu | \mu \in L^\infty(t_0, t_f; \mathbf{R}^d), \|\mu(t)\|_{\mathbf{R}^d} \leq 1, \ a.e. \ on \ (t_0, t_f)\}$. Combining (26) and (36), with the fact that $\tilde{\Lambda}$ is compact for the weak-* topology of $L^\infty(t_0, t_f; \mathbf{R}^d)$, we can prove (relatively easily) that $\lim_{\tau_1 \to 0} \lambda_{\tau_1} = \lambda$ in $L^\infty(t_0, t_f; \mathbf{R}^d)$ weak-*. Improving over the above convergence result is difficult since λ^p in (26) is a subgradient at W^p of the functional $j(.)$ defined by (28), i.e. $\lambda^p = \partial j(W^p)$, with the subgradient operator $\partial j(.)$ *multivalued*, i.e. *discontinuous*.

Remark 3.2: Suppose that problem (24) is a sub-problem coming from the time-discretization by operator-splitting of an initial value problem such as (1). Then, we have, typically, $t_0 = t^n (= n\Delta t)$ and $t_f = t^{n+1} (= (n+1)\Delta t)$. There is, clearly, no ambiguity concerning the definition of $X^{n+1/2}$ and $V^{n+1/2}$. On the other hand, we have to be

careful when defining the friction multiplier $\lambda^{n+1/2}$; actually, a close inspection shows that we should define $\lambda^{n+1/2}$ by

$$\lambda^{n+1/2} = (\sum_{p=1}^{P} \lambda^{n+1/2,p})/P, \tag{37}$$

where $\{\lambda^{n+1/2,p}\}_{p=1}^{P}$ is the set of the friction multipliers encountered when solving problem (10) via scheme (25), (26). ♢

3.2. Iterative Solution of System (27)

Dropping the superscripts p, problem (27) takes the following form:

$$\begin{cases} MW + \tau_1 C\ \lambda = b, \\ C\ \lambda \cdot W = \sum_{i=1}^{d} c_i |w_i|, \quad \lambda \in \Lambda. \end{cases} \tag{38}$$

If $d = 1$ computing the *closed form solution* of problem (38) is quite easy (see Remarks 3.3 below). On the other hand, if $d \geq 2$, then we must rely on *iterative techniques*. A simple one is provided by the following algorithm

$$\lambda^0 \ \text{ given in } \ \Lambda; \tag{39}$$

for $k \geq 0$, λ^k *being known, solve*

$$MW^k = b - \tau_1 C\lambda^k \tag{40}$$

and update λ^k *via*

$$\lambda^{k+1} = P_\Lambda(\lambda^k + \rho C W^k). \tag{41}$$

In (41), the *projection* operator $P_\Lambda : \mathbf{R}^d \to \Lambda$ is defined by

$$P_\Lambda(\mu) = \{min(1, max(-1, \mu_i))\}_{i=1}^{d},\ \forall \mu = \{\mu_i\}_{i=1}^{d} \in \mathbf{R}^d. \tag{42}$$

Set Λ being closed, convex (and non-empty), operator P_Λ is a *contraction*. Concerning the convergence of algorithm (39)-(41), we then have the following

Theorem 3.2 *Suppose that*

$$0 < \rho < \frac{2}{\tau_1 \beta_d}, \tag{43}$$

where β_d *is the largest eigenvalue of matrix* $M^{-1}C^2$*; we have then,* $\forall \lambda^0 \in \Lambda$,

$$\lim_{k \to +\infty} \{W^k, \lambda^k\} = \{W, \lambda\}, \tag{44}$$

where $\{W, \lambda\}$ *is the solution of system (38).*

Proof: : The proof is a fairly classical one (see, e.g.,[5] and the references therein). In order to avoid tedious reference consultation by the readers, we are going to give this proof *in extenso* in this article. The key point is to observe that an *equivalent* formulation of (38) is given by

$$\begin{cases} MW + \tau_1 C\ \lambda = b \\ \lambda = P_\Lambda(\lambda + \rho C W), \quad \forall \rho > 0. \end{cases} \tag{45}$$

Showing that (45) holds is very easy: we have, from (38),

$$\begin{aligned} CW \cdot (\mu - \lambda) &= CW \cdot \mu - \sum_{i=1}^{d} c_i |w_i| \\ &= \sum_{i=1}^{d} c_i \mu_i w_i - \sum_{i=1}^{d} c_i |w_i| \\ &\leq \sum_{i=1}^{d} c_i |\mu_i| |w_i| - \sum_{i=1}^{d} c_i |w_i| \\ &\leq \sum_{i=1}^{d} c_i |w_i| - \sum_{i=1}^{d} c_i |w_i| = 0, \ \forall \mu \in \Lambda. \end{aligned}$$

Relation $CW \cdot (\mu - \lambda) \leq 0, \forall \mu \in \Lambda$, implies

$$\begin{cases} (\lambda + \rho CW - \lambda) \cdot (\mu - \lambda) \leq 0, \forall \mu \in \Lambda, \forall \rho > 0, \\ \lambda \in \Lambda. \end{cases}$$

We have thus (see, e.g., [11])

$$\lambda = P_\Lambda(\lambda + \rho CW), \forall \rho > 0. \tag{46}$$

Conversely, if the equation in (46) holds for an arbitrary positive value of ρ, then (38) takes place, justifying therefore replacing (38) by (45). Denote $W^k - W$ and $\lambda^k - \lambda$ by $\overline{W}^k$ and $\overline{\lambda}^k$, respectively. Since operator P_Λ is a contraction it follows from (40), (41) and (45) that

$$M\overline{W}^k = -\tau_1 C\overline{\lambda}^k \tag{47}$$

and

$$\|\overline{\lambda}^{k+1}\|_{\mathbf{R}^d} \leq \|\overline{\lambda}^k + \rho C\overline{W}^k\|_{\mathbf{R}^d}. \tag{48}$$

Combining (47) with (48), we obtain

$$\|\overline{\lambda}^k\|^2_{\mathbf{R}^d} - \|\overline{\lambda}^{k+1}|^2_{\mathbf{R}^d} \geq 2\rho\tau_1^{-1} M\overline{W}^k \cdot \overline{W}^k - \rho^2 \|C\overline{W}^k\|^2_{\mathbf{R}^d}. \tag{49}$$

Recall that $\|CV\|^2 \leq \beta_d MV \cdot V, \ \forall V \in \mathbf{R}^d$, with β_d the largest eigenvalue of $M^{-1}C^2$. It follows then from (49) that

$$\|\overline{\lambda}^k\|^2_{\mathbf{R}^d} - \|\overline{\lambda}^{k+1}|^2_{\mathbf{R}^d} \geq \rho(2/\tau_1 - \rho\beta_d) M\overline{W}^k \cdot \overline{W}^k. \tag{50}$$

Suppose that condition (43) holds. It follows from (50) and from the positivity of matrix M that the sequence $\{\|\overline{\lambda}^k\|^2_{\mathbf{R}^d}\}_{k\geq 0}$, is *decreasing*; since it has 0 as lower bound, it converges implying that $\lim(\|\overline{\lambda}^k\|^2_{\mathbf{R}^d} - \|\overline{\lambda}^{k+1}|^2_{\mathbf{R}^d}) = 0$, which implies in turn that $\lim_{k\to+\infty} W^k = W$ and (from (47)) that $\lim_{k\to+\infty} \lambda^k = \lambda$. The convergence result (44) has been proved.

Remark 3.3: Suppose that $d = 1$; with obvious notation, problem (26) reduces to

$$\begin{cases} mw^p + \tau_1 c\lambda^p = mw^{p-1} + \tau_1 c\gamma(w^{p-1}) + \tau_1 f^p, \\ \lambda^p w^p = |w^p|, \quad |\lambda^p| \leq 1. \end{cases} \tag{51}$$

An alternative formulation is given by

$$mw^p + \tau_1 csgn(w^p) = mw^{p-1} + \tau_1 c\gamma(w^{p-1}) + \tau_1 f^p. \tag{52}$$

Function $\xi \rightarrow m\xi + c\tau_1 sgn(\xi)$ being strictly monotone with range $\mathbf{R}$, problems (51) and (52) have unique solutions, $\forall \tau_1 (\leq t_f - t_0)$; we have

$$\begin{cases} w^p = 0 \ \text{ if } \ |b^p| \leq c\tau_1, \\ w^p = (b^p - c\tau_1 sgn(b^p))/m \ \text{ if } \ |b^p| \geq c\tau_1, \end{cases} \tag{53}$$

with $b^p = mw^{p-1} + c\tau_1\gamma(w^{p-1}) + \tau_1 f^p$. Once w^p is known, we obtain λ^p from the first equation in (51) followed by a "projection" on the interval $[-1, 1]$. Actually, some important applications take place in one-space dimension; one of them is the so-called "gear box efficiency problem", a variant of problem (24) defined as follows:

$$\begin{cases} m\dot{w} + c(sgn(w) - \gamma(w)) + k(\delta)g(\delta w) = f \quad \text{on} \quad (t_0, t_f), \\ w(t_0) = w_0, \end{cases} \tag{54}$$

where in (54): (i) Parameter δ is given in $\mathbf{R}$. (ii) $k(\cdot)$ is an increasing odd function of δ vanishing at 0 and Lipschitz continuous over $\mathbf{R}$. (iii)Function g is of the following form:

$$g(\xi) = \frac{a+b}{2} + \frac{b-a}{2}[sgn(\xi) - \gamma_{ab}(\xi)]$$

with $0 < a < b$ and function γ_{ab} of the same type than γ (see Section 2 for details). The *monotonicity*, $\forall \delta \in \mathbf{R}$, of operator $w \rightarrow k(\delta)sgn(\delta w)$, is the property making the above generalization possible.

Remark 3.4: Numerical experiments show that algorithm (39)-(41) performs slowly, in general. In order to speed-up the solution of the pure friction problems, we will introduce in Section 6 a penalty/Newton method closely related to the one discussed in [13] and [14] for the solution of time dependent obstacle problems.

4. Numerical solution of type (12), (14) subproblems

Problems (12),(14) are very classical ones. We shall briefly discuss their solution by (well-known) finite difference schemes. Let Q be a positive integer and denote $\Delta t/Q$ by τ_2. With obvious notation (and $0 \leq \alpha \leq 1/2$), we approximate problem (14) by

$$X^{n+1,0} = X^{n+1/2}, \quad X^{n+1,1} - X^{n+1,-1} = 2\tau_2 V^{n+1/2}; \tag{55}$$

for $q = 0, \cdots, Q$, $X^{n+1,q}$ and $X^{n+1,q-1}$ being known, solve:

$$\begin{aligned} & M\frac{X^{n+1,q+1} + X^{n+1,q-1} - 2X^{n+1,q}}{\tau_2^2} \\ + \quad & A(\alpha X^{n+1,q+1} + (1-2\alpha)X^{n+1,q} + \alpha X^{n+1,q-1}) = 0, \end{aligned} \tag{56}$$

$$X^{n+1} = X^{n+1,Q}, \quad V^{n+1} = (X^{n+1,Q+1} - X^{n+1,Q-1})/2\tau_2. \tag{57}$$

It is well known (see, e.g., [1], [2], [12] and the references therein) that scheme (55), (56) is *unconditionally stable* if $1/4 \leq \alpha \leq 1/2$; if $0 \leq \alpha < 1/4$, one has stability provided that $\tau_2 < 1/\sqrt{(1/4 - \alpha)\nu_d}$, ν_d being the largest eigenvalue of matrix $M^{-1}A$ (i.e., $\tau_2 < 2/\sqrt{\nu_d}$ if $\alpha = 0$).

5. Numerical experiments

In order to validate the methodology discussed in the above sections, we are going to apply it to four test problems. The first two test problems correspond to $d = 1$, while the third one corresponds to $d = 2$ and the fourth one corresponds to $d = 3$. These four test problems all have closed form solutions.

5.1. First test problem

The *pure friction* problem that we consider is a particular case of problem (24) which reads as follows:

$$\begin{cases} m\dot{w} + c(sgn(w) - \gamma(w)) = f \quad \text{on } (t_0, t_f), \\ w(t_0) = w_0, \end{cases} \tag{58}$$

or (preferably)

$$\begin{cases} m\dot{w} + c(\lambda - \gamma(w)) = f \quad \text{on } (t_0, t_f), \\ \lambda w = |w|, |\lambda| \leq 1 \quad \text{on } (t_0, t_f), \\ w(t_0) = w_0. \end{cases} \tag{59}$$

The numerical experiments have been carried out with $t_0 = 0, t_f = 2, m = 1, c = 0.5, w_0 = 0$, and γ defined by (3) with $\beta = 1/3$ and $\epsilon = 1/10$; the forcing term is given by

$$f(t) = \begin{cases} 2\pi m cos2\pi t + c[1 - \gamma(sin2\pi t)] & \text{if } t \in (0, 1/2) \cup (1, 3/2), \\ 0 & \text{if } t \in (1/2, 1) \cup (3/2, 2). \end{cases}$$

With such f and w_0, the unique solution of problem (58), (59) is given by $w(t) = (sin2\pi t)^+ (= max(0, sin2\pi t)), \forall t \in [0, 2]$, and $\lambda(t) = 1$ if $t \in (0, 1/2) \cup (1, 3/2)$, $\lambda(t) = 0$ if $t \in (1/2, 1) \cup (3/2, 2)$. On figure 1, we have shown the graphs of the approximate w computed with $\Delta t = 10^{-2}$ and 10^{-3}. On figure 2, we have shown the graphs of the approximated friction multiplier λ (as defined in Remark 3.1) computed for the two different values of Δt. Finally, on figure 3, we have represented on a log-scale the variation of the L^2-approximation error on w as a function of Δt; this figure clearly "suggests" *first order accuracy*, for this test problem at least (the convergence of λ is obviously not as good).

5.2. Second test problem

The second test problem that we consider is defined by

$$\begin{cases} m\ddot{x} + kx + c(sgn(\dot{x}) - \gamma(\dot{x})) = f \quad \text{on } (t_0, t_f), \\ x(t_0) = x_0, \ \dot{x}(t_0) = v_0. \end{cases} \tag{60}$$

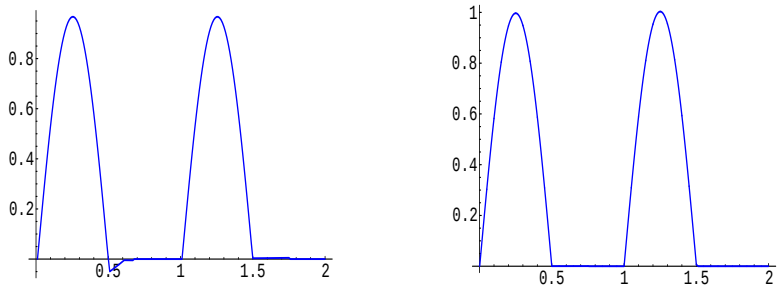

Figure 1. Test prob. 1: (left) the computed $w(t)$ with $\Delta t = 10^{-2}$; (right) the computed $w(t)$ with $\Delta t = 10^{-3}$

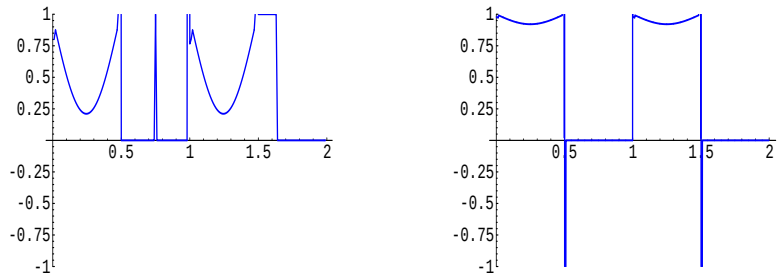

Figure 2. Test prob. 1: (left) the computed $\lambda(t)$ with $\Delta t = 10^{-2}$; (right) the computed $\lambda(t)$ with $\Delta t = 10^{-3}$

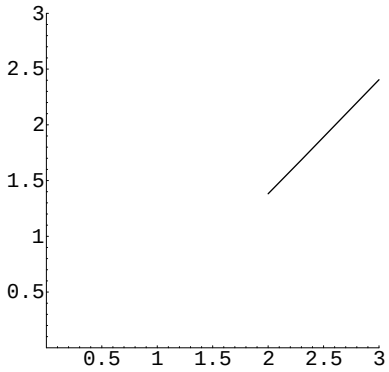

Figure 3. Test prob. 1: variation of the L^2-error on w versus Δt in log-scale

In (60), we take $t_0 = 1, t_f = 3, m = 1, c = 0.2, k = 1, x_0 = 0, v_0 = 0$ and γ is as in Section 5.1; this time, the forcing term is given by

$$f(t) = \begin{cases} 8m\pi^2 cos4\pi t + ksin^2 2\pi t + c[1 - \gamma(2\pi sin4\pi t)], & \text{if } t \in (1, 5/4) \cup (2, 9/4), \\ 8m\pi^2 cos4\pi t + ksin^2 2\pi t - c[1 + \gamma(2\pi sin4\pi t)], & \text{if } t \in (5/4, 3/2) \cup (9/4, 5/2), \\ -c/2 & \text{if } t \in (3/2, 2) \cup (5/2, 3). \end{cases}$$

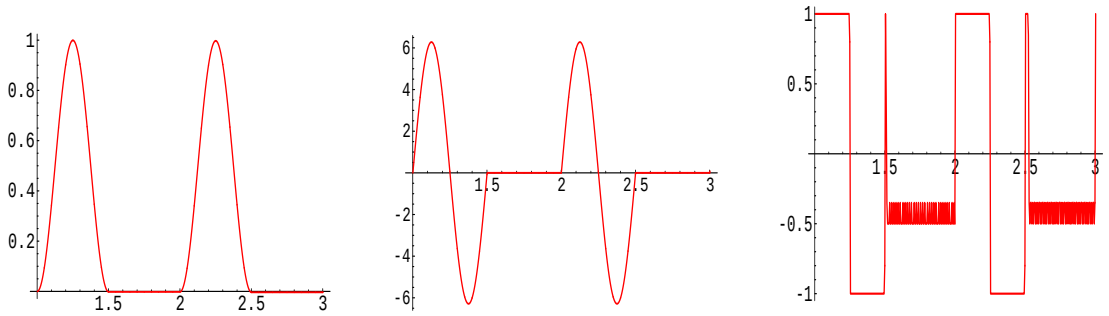

Figure 4. Test prob. 2: (left) the computed $x(t)$; (middle) the computed $v(t) = \dot{x}$; (right) the computed $\lambda(t)$

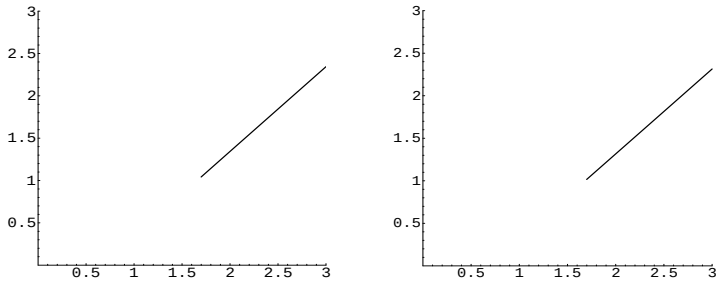

Figure 5. Test prob. 2: (left) L^2-error on x: variation versus Δt in log-scale; (right) L^2-error on v: variation versus Δt in log-scale

For the above data, the solution of problem (60) is given by $x(t) = (sin2\pi t)^{+2}, \forall t \in [1,3]$, while the corresponding function λ is given by

$$\lambda(t) = \begin{cases} 1, & \text{if } t \in (1,5/4) \cup (2,9/4), \\ -1, & \text{if } t \in (5/4,3/2) \cup (9/4,5/2), \\ -\frac{1}{2}, & \text{if } t \in (3/2,2) \cup (5/2,3). \end{cases}$$

To solve problem (60), we have used the splitting scheme (9)− (13), the subproblems (10) and (12) being solved via schemes (25), (26) and (55)− (57), respectively. The following results have been obtained with $\tau_1 = \Delta t/10$ and $\tau_2 = \Delta t/2$. On figure 4 , we have shown the graphs of the approximation of $x, \dot{x}$, and λ, respectively, all obtained with $\Delta t = 10^{-3}$. On figure 5, we have shown the L^2-error, in x and $\dot{x}$, as functions of Δt in log-scale. As in Section 5.1, we still have *first order accuracy.*

5.3. Third test problem

The third test problem is multidimensional with $d = 2$. It is defined as follows:

$$\begin{cases} M\ddot{X} + AX + C(\lambda - \gamma(\dot{X})) = f \quad \text{on } (t_0, t_f), \\ |\lambda_i| \leq 1, \ \ \forall i = 1,2, \ \ \lambda \cdot \dot{X} = |\dot{X}|, \\ X(0) = X_0, \ \ \dot{X}(0) = V_0, \end{cases} \tag{61}$$

with

- $M = \begin{pmatrix} 2 & 1 \\ 1 & 2 \end{pmatrix}$, $A = \begin{pmatrix} 2 & -1 \\ -1 & 2 \end{pmatrix}$, $C = I$,
- $\gamma = 0$,
- $f = \{f_i\}_{i=1}^2$, where

$$f_1(t) = \begin{cases} 2(t - \frac{t^2}{2}) - 1 & \text{if } 0 \le t \le 1, \\ 1 + (t - \frac{3}{2}) & \text{if } 1 \le t \le 2, \\ 3t^3 - 23t^2 + 70t - \frac{238}{3} & \text{if } 2 \le t \le 3, \\ \frac{t^3}{3} - 3t^2 + 6t - \frac{17}{6} & \text{if } 3 \le t \le 4, \end{cases}$$

and

$$f_2(t) = \begin{cases} \frac{t^2}{2} - 2t & \text{if } 0 \le t \le 1, \\ \frac{1}{2} - t & \text{if } 1 \le t \le 2, \\ -2t^3 + 16t^2 - 36t + \frac{163}{6} & \text{if } 2 \le t \le 3, \\ \frac{-2}{3}t^3 + 6t^2 - 20t + \frac{175}{6} & \text{if } 3 \le t \le 4. \end{cases}$$

- $X_0 = \{0, 0\},\ V_0 = \{1, 0\}$.

For the above data, the solution of problem (61) is given by

$$x_1(t) = \begin{cases} t - \frac{t^2}{2} & \text{if } 0 \le t < 1, \\ \frac{1}{2} & \text{if } 1 \le t < 2, \\ \frac{1}{2} + 4[\frac{1}{3}(t^3 - 8) - \frac{5}{2}(t^2 - 4) + 6(t - 2)] & \text{if } 2 \le t < 3, \\ \frac{-1}{6} & \text{if } 3 \le t \le 4, \end{cases}$$

and

$$x_2(t) = \begin{cases} 0 & \text{if } 0 \le t < 2, \\ (t - 2) - \frac{1}{3}((t - 3)^3 + 1) & \text{if } 2 \le t \le 4, \end{cases}$$

while the corresponding function λ is given by

$$\lambda_1(t) = \begin{cases} 1 & \text{if } 0 \le t < 1, \\ t - \frac{3}{2} & \text{if } 1 \le t \le 2, \\ -1 & \text{if } 2 < t < 3, \\ \frac{-1}{2} & \text{if } 3 < t < 4. \end{cases}$$

and

$$\lambda_2(t) = \begin{cases} 1 - t & \text{if } 0 \le t \le 2, \\ 1 & \text{if } 2 \le t \le 4. \end{cases}$$

To solve problem (61), we have used the splitting scheme (9)−(13), the subproblems (10) and (12) being solved via schemes (25), (26) and (55)−(57), respectively. The following results have been obtained with $\tau_1 = \Delta t/10$, and $\tau_2 = \Delta t/2$. On figures 6-8, we have shown the graphs of the approximation of λ, $\dot{X}$, and X, respectively, all obtained with $\Delta t = 10^{-3}$.

For the same data, let $\gamma = \{\gamma_i\}_{i=1}^2$ be defined as in (3), with $\beta_i = \frac{1}{3}$ and $\epsilon_i = 10^{-2}, i = 1, 2$. We then have the solutions visualized in figures 9-11. We observe that the computed discrete multipliers do not exhibit spurious oscillation, as it is the case with other discretization schemes (see ref. [1]). Finally, we have shown in figure 12 the variation of the approximation error on X, V, λ as functions of Δt in log-scale.

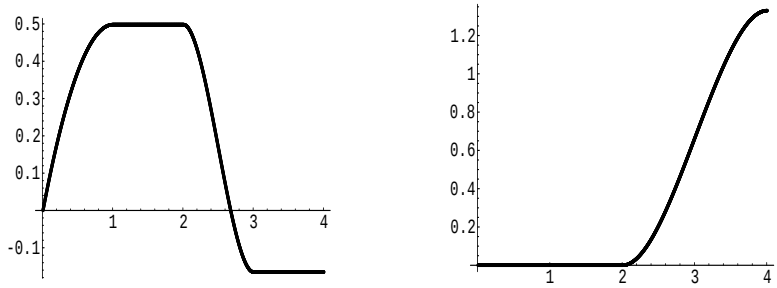

Figure 6. Test prob. 3 ($\gamma = 0$): (left) the computed x_1; (right) the computed x_2

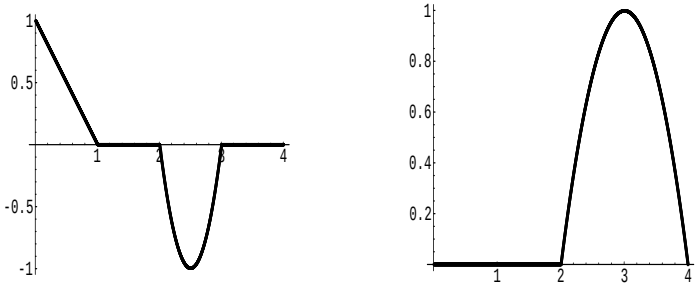

Figure 7. Test prob. 3 ($\gamma = 0$):(left) the computed v_1; (right) the computed v_2

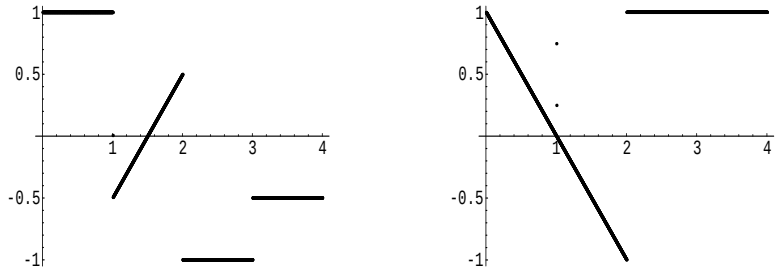

Figure 8. Test prob. 3 ($\gamma = 0$):(left) the computed $\lambda_1(t)$; (right) the computed $\lambda_2(t)$

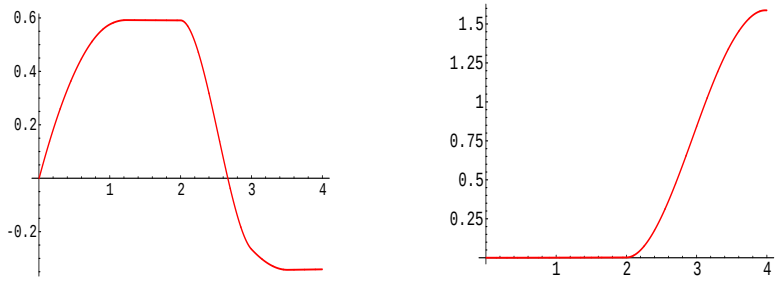

Figure 9. Test prob. 3 ($\gamma \neq 0$):(left) the computed $x_1(t)$; (right) the computed $x_2(t)$

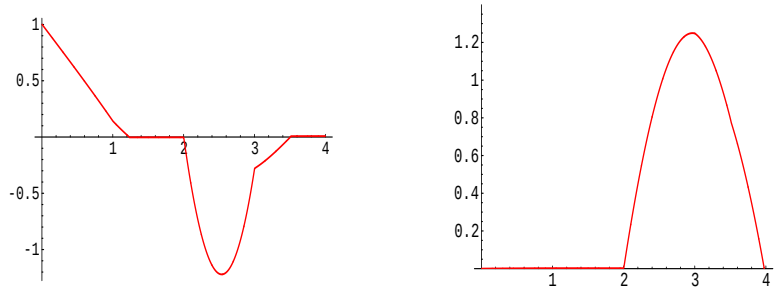

Figure 10. Test prob. 3 ($\gamma \neq 0$):(left) the computed $v_1(t)$; (right) the computed $v_2(t)$

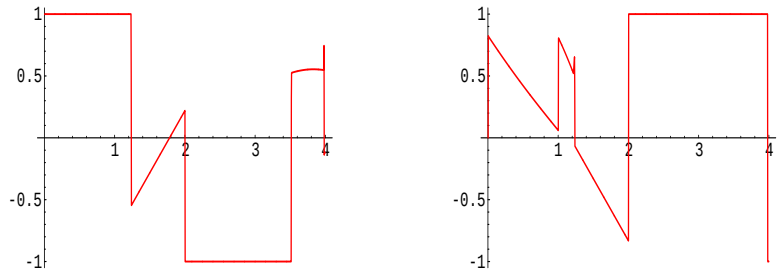

Figure 11. Test prob. 3 ($\gamma \neq 0$):(left) the computed $\lambda_1(t)$; (right) the computed $\lambda_2(t)$

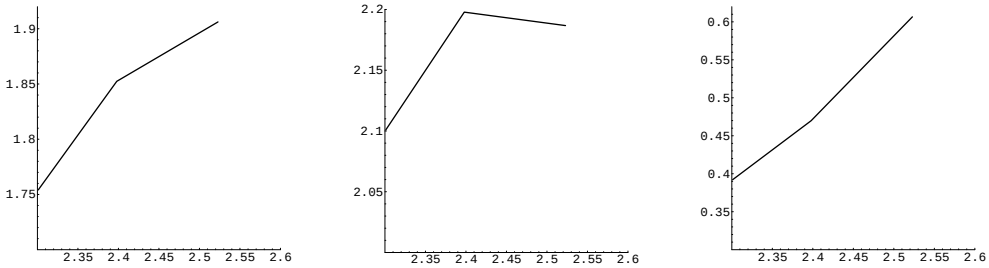

Figure 12. Test prob. 3 ($\gamma \neq 0$): (left) L^2-error on $\dot{X}$ versus τ in log-scale; (middle) L^2-error on X versus τ in log-scale; (right) L^2-error on λ versus τ in log-scale

5.4. Fourth test problem

We will describe in this section the numerical results obtained when applying the methodology of the previous sections to a *3-degree of freedom* model problem (1),(4). We take $T = 4$ and

- the mass matrix $M = \begin{pmatrix} 1 & 0 & 0 \\ 0 & 2 & 0 \\ 0 & 0 & 3 \end{pmatrix}$, the friction matrix $C = 10I$, the stiffness matrix $A = \mathbf{0}$ and $\gamma = \mathbf{0}$,
- the external forcing term $f = \{f_i\}_{i=1}^3$, where $f_i(t) = -20e^{-4t}$.
- $X_0 = \{1, 2, 3\}$, $V_0 = \{1, 1, 1\}$.

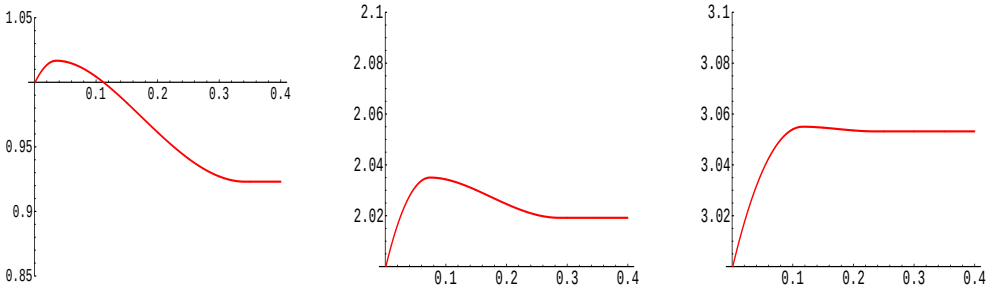

Figure 13. Test prob. 4: (left) the computed $x_1(t)$; (middle) the computed $x_2(t)$; (right) the computed $x_3(t)$

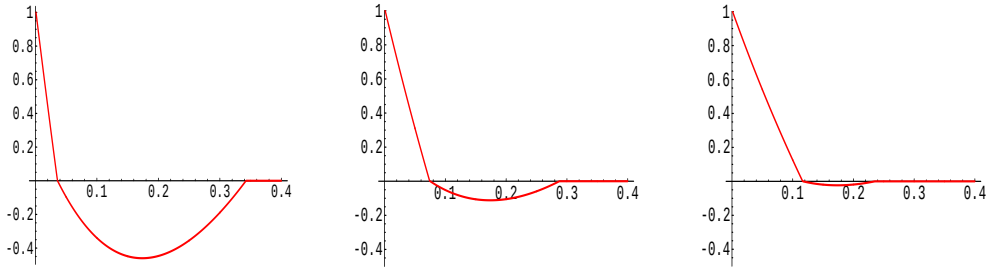

Figure 14. Test prob. 4: (left) the computed $v_1(t)$; (middle) the computed $v_2(t)$; (right) the computed $v_3(t)$

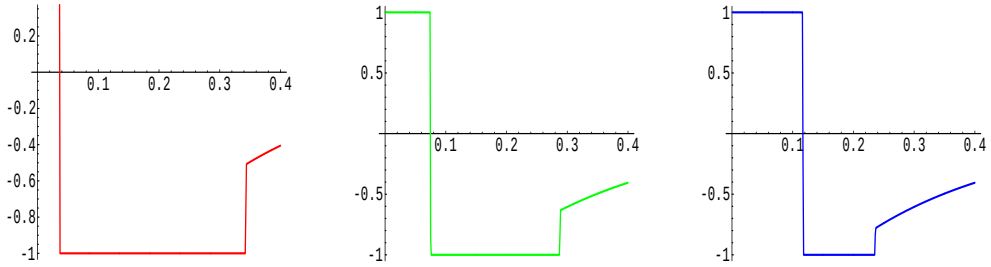

Figure 15. Test prob. 4: (left) the computed $\lambda_1(t)$; (middle) the computed $\lambda_2(t)$; (right) the computed $\lambda_3(t)$

To solve problem (1), we have used the same schemes and steps as for the second test problem. On figures 13-15, we have shown the graphs of the approximation of $\dot{X}$, X, λ, respectively, obtained using $\Delta t = 0.003$. Based on the previous two test problems, a first order accuracy is expected for this test problem as well. As in Section 5.3, we observe that the computed discrete multipliers do not exhibit spurious oscillations.

5.5. Comments on the convergence of algorithm (39)-(41)

While reporting the numerical experiments whose results are shown in Sections 5.3 and 5.4, we did not provide the number of iterations of algorithm (39)-(41) that it takes to

solve the problems (26). Actually, "most of the time", algorithm (39)-(41) performed slowly (more than one hundred iterations was not uncommon). In order to achieve faster convergence in the solution of problems (26), we are going to apply a variant of the penalty/Newton methodology discussed in [13] and [14] (for the solution of time dependent obstacle problems).

6. A penalty/Newton method for the solution of problems (26)

6.1. Reduction to an obstacle problem in $\mathbf{R}^d$

All the problems (26) being particular cases of problem (38), we will focus on the solution of this last problem. First of all, we observe that problem (38) is equivalent to

$$\left\{ \begin{array}{l} \{W, \lambda\} \in \mathbf{R}^d \times \Lambda, \\ MW + \tau_1 C\lambda = b, \\ -CW \cdot (\mu - \lambda) \geq 0, \ \forall \mu \in \Lambda. \end{array} \right. \tag{62}$$

Eliminating W from (62), we obtain the following equivalent variational formulation of problem (38)

$$\left\{ \begin{array}{l} \lambda \in \Lambda, \\ \tau_1 CM^{-1}C\lambda \cdot (\mu - \lambda) \geq CM^{-1}b \cdot (\mu - \lambda), \ \forall \mu \in \Lambda. \end{array} \right. \tag{63}$$

Problem (63) is an obstacle problem in $\mathbf{R}^d$; it belongs to the class finite or infinite dimensional variational inequalities discussed in, e.g., [3], [5] and [16]. The numerical solution of discrete obstacle problems such as (63) has motivated a huge literature. Considering the time dependent nature of the problem leading to (38), we are going to apply to the solution of this last problem the penalty/Newton methodology developed in [13] (see also [14]) for the solution of parabolic variational inequalities of the obstacle type. Penalty techniques have also been applied to the solution of obstacle problem in Finite Elasticity (see, e.g., [15] and the references therein).

From now on, we will denote the symmetric positive definite matrix $\tau_1 CM^{-1}C$ by $\mathcal{A}$ and the vector $CM^{-1}b$ by β. Problem (63) takes then the following form

$$\left\{ \begin{array}{l} \lambda \in \Lambda, \\ \mathcal{A}\lambda \cdot (\mu - \lambda) \geq \beta(\mu - \lambda), \ \forall \mu \in \Lambda. \end{array} \right. \tag{64}$$

The matrix $\mathcal{A}$ being symmetric and positive definite, problem (64) is equivalent to

$$\left\{ \begin{array}{l} \lambda \in \Lambda, \\ j(\lambda) \leq j(\mu), \ \forall \mu \in \Lambda, \end{array} \right. \tag{65}$$

with the functional $j : \mathbf{R}^d \mapsto \mathbf{R}$ defined by

$$j(\mu) = \frac{1}{2}\mathcal{A}\mu \cdot \mu - \beta \cdot \mu, \ \forall \mu \in \mathbf{R}^d. \tag{66}$$

6.2. Penalty approximation of problem (64),(65)

Following [13] and [14], we use penalty to approximate problem (64),(65) by

$$\begin{cases} \lambda_\epsilon \in \mathbf{R}^d, \\ j_\epsilon(\lambda_\epsilon) \leq j_\epsilon(\mu), \ \forall \mu \in \mathbf{R}^d, \end{cases} \tag{67}$$

with ϵ a "small" positive parameter and

$$j_\epsilon(\mu) = j(\mu) + \frac{1}{3\epsilon} \sum_{i=1}^{d} [((\mu_i - 1)^+)^3 + ((\mu_i + 1)^-)^3], \tag{68}$$

we recall that $\xi^+ = max(0, \xi)$, $\xi^- = -min(0, \xi)$. The function j_ϵ being strictly convex,C^2 and verifying $\lim_{\|\mu\| \mapsto +\infty} j_\epsilon(\mu) = +\infty$, problem (67) has a unique solution characterized by

$$j'_\epsilon(\lambda_\epsilon) = 0, \tag{69}$$

with $j'_\epsilon(.)$ the differential of the function of $j_\epsilon(.)$. Namely,

$$j'_\epsilon(\mu) = \mathcal{A}\mu - \beta + \frac{1}{\epsilon}[((\mu - 1)^+)^2 - ((\mu + 1)^-)^2], \ \forall \mu \in \mathbf{R}^d, \tag{70}$$

where $((\mu - 1)^+)^2$ (respectively $((\mu + 1)^-)^2$) is a symbolic notation for the vector $\{((\mu_i - 1)^+)^2\}_{i=1}^d$ (respectively $\{((\mu_i + 1)^+)^2\}_{i=1}^d$). The solution of the nonlinear system (69) will be discussed in the following section.

6.3. A Newton's algorithm for the solution of problem (69)

Let us denote $j'_\epsilon(\cdot)$ by $F_\epsilon(\cdot)$, implying that the nonlinear system (69) reads now as follows:

$$F_\epsilon(\lambda_\epsilon) = 0. \tag{71}$$

In order to solve problem (71), we will use a Newton's algorithm as advocated in [13], [14] for other obstacle problems. It follows from, e.g., [17] that a Newton's algorithm for the solution of problem (71) is given by:

$$\lambda_\epsilon^0 \in \mathbf{R}^d; \tag{72}$$

for $k \geq 0$, λ_ϵ^k being known, we obtain λ_ϵ^{k+1} from:

$$\lambda_\epsilon^{k+1} = \lambda_\epsilon^k - (F'_\epsilon(\lambda_\epsilon^k))^{-1} F_\epsilon(\lambda_\epsilon^k); \tag{73}$$

In (73), the *matrix-valued function* F'_ϵ is defined by

$$F'_\epsilon(\mu) = \mathcal{A} + \frac{2}{\epsilon}[(\mu - 1)^+ + (\mu + 1)^-], \ \forall \mu \in \mathbf{R}^d, \tag{74}$$

where, in (74), $(\mu - 1)^+$ (resp., $(\mu + 1)^-$) is a symbolic notation for the *diagonal matrix*

$$\begin{pmatrix} (\mu_1 - 1)^+ & & & & 0 \\ & \ddots & & & \\ & & (\mu_i - 1)^+ & & \\ & & & \ddots & \\ 0 & & & & (\mu_d - 1)^+ \end{pmatrix}$$

(resp.,

$$\begin{pmatrix} (\mu_1+1)^- & & & & 0 \\ & \ddots & & & \\ & & (\mu_i+1)^- & & \\ & & & \ddots & \\ 0 & & & & (\mu_d+1)^- \end{pmatrix}$$

). The two above diagonal matrices are positive semi-definite, matrix $F'_\epsilon(\mu)$ is positive symmetric and positive definite, for all $\mu \in \mathbf{R}^d$, which implies in turn that one can use the method of Cholesky to compute the vector $(F'_\epsilon(\lambda^k_\epsilon))^{-1}F(\lambda^k_\epsilon)$. Concerning the choice of λ^0_ϵ in the context of the solution of problem (26), we advocate taking for λ^0_ϵ the multiplier solution at the previous time step. The convergence of Newton's algorithms such as (72) and (73) is discussed in [17].

6.4. Numerical Experiments

6.4.1. Fifth test problem The fifth test problem is also multidimensional with $d = 3$; it is defined as follows:

$$\begin{cases} M\ddot{X} + AX + C(\lambda - \gamma(\dot{X})) = f \qquad \text{on } (t_0, t_f), \\ |\lambda_i| \le 1, \ \ \forall i = 1,2,3, \ \lambda \cdot \dot{X} = |\dot{X}|, \\ X(0) = X_0, \ \dot{X}(0) = V_0, \end{cases} \tag{75}$$

with

- $M = \begin{pmatrix} 2 & 1 & 0 \\ 1 & 2 & 1 \\ 0 & 1 & 1 \end{pmatrix}$, $A = \begin{pmatrix} 2 & -1 & 0 \\ -1 & 2 & -1 \\ 0 & -1 & 2 \end{pmatrix}$, $C = I$,
- $\gamma \neq 0$, as previously defined in (3),
- $f = \{f_i\}_{i=1}^3$, where

$$f_1(t) = \begin{cases} -1 + 2t - t^2 - \gamma(1-t) & \text{if } \ 0 \le t \le 1, \\ 1 + (t - \frac{3}{2}) - \gamma(0) & \text{if } \ 1 \le t \le 2, \\ -78 + 70t - 23t^2 + 3t^3 - \gamma(4(t-3)(t-2)) & \text{if } \ 2 \le t \le 3, \\ -1 - \frac{1}{2} - 3t^2 + 6t + \frac{t^3}{3} - \gamma(0) & \text{if } \ 3 \le t \le 4, \end{cases}$$

$$f_2(t) = \begin{cases} -t + \frac{t^2}{2} - \gamma(0) & \text{if } \ 0 \le t \le 1, \\ 2t - 2t - \frac{t^2}{2} - \gamma(0) & \text{if } \ 1 \le t \le 2, \\ -2t^3 + 16t^2 - 36t + 26 - \gamma(1 - (t-3)^2) & \text{if } \ 2 \le t \le 3, \\ 10 - 5t + 2t^2 - \frac{t^3}{3} - \gamma(1 - (t-3)^2) & \text{if } \ 3 \le t \le 4, \end{cases}$$

and

$$f_3(t) = \begin{cases} -1 - 2t - \gamma(t-2) & \text{if } \ 0 \le t \le 1, \\ 1 - 4t + t^2 - \gamma(t-2) & \text{if } \ 1 \le t \le 2, \\ \frac{-14 + 18t - 9t^2 + t^3}{3} - \gamma(0) & \text{if } \ 2 \le t \le 3, \\ \frac{106}{3} - 24t + 5t^2 - \frac{t^3}{3} - \gamma(1 - (t-4)^2) & \text{if } \ 3 \le t \le 4. \end{cases}$$

- $X_0 = \{0, 0, 0\},\ V_0 = \{1, 0, -1\}$.

With these data, the exact solution of this test problem is given by:

$$x_1(t) = \begin{cases} 1-t & \text{if } 0 \le t < 1, \\ 0 & \text{if } 1 \le t < 2, \\ 4(t-3)(t-2) & \text{if } 1 \le t < 2, \\ 0 & \text{if } 2 \le t < 3, \end{cases}$$

$$x_2(t) = \begin{cases} 0 & \text{if } 0 \le t < 2, \\ 1-(t-3)^2 & \text{if } 2 \le t < 4, \end{cases}$$

and

$$x_3(t) = \begin{cases} -1 & \text{if } 0 \le t < 1, \\ t-2 & \text{if } 1 \le t < 2, \\ 0 & \text{if } 1 \le t < 2, \\ 1-(t-4)^2 & \text{if } 2 \le t < 3, \end{cases}$$

while the corresponding function λ is given by

$$\lambda_1(t) = \begin{cases} 1 & \text{if } 0 \le t < 1, \\ t-\frac{3}{2} & \text{if } 1 \le t \le 2, \\ -1 & \text{if } 2 < t < 3, \\ \frac{-1}{2} & \text{if } 3 < t < 4, \end{cases}$$

$$\lambda_2(t) = \begin{cases} 1-t & \text{if } 0 \le t < 2, \\ 1 & \text{if } 3 \le t \le 4, \end{cases}$$

and

$$\lambda_3(t) = \begin{cases} -1 & \text{if } 0 \le t \le 2, \\ (5-2t) & \text{if } 2 \le t \le 3, \\ 1 & \text{if } 3 \le t \le 4. \end{cases}$$

Taking $V = \dot{X}$ as unknown function, problem (75) reads as follows:

$$\begin{cases} M\dot{V} + AX + C(\lambda - \gamma(V)) = f & \text{on } (0,T), \\ \dot{X} = V & \text{on } (0,T), \\ |\lambda_i| \le 1, \ \ \forall i = 1,2,3, \ \lambda \cdot V = |V|, \\ X(0) = X_0, \ V(0) = V_0. \end{cases} \tag{76}$$

Scheme (9)−(13), with $T = 4$ and $\Delta t = 0.008$, was applied to the solution of problem (76), the corresponding problems (26) being solved by the penalty/Newton method discussed above with $\epsilon = 10^{-4}$. No more than 4 Newton's iterations were required at each time-step, making this approach much faster than the one based on algorithm (39)−(41). The results are reported in figures, where we show the graphs of the computed x_1, x_2, x_3 (figure 16), v_1, v_2, v_3 (figure 17) and of $\lambda_1, \lambda_2, \lambda_3$ (figure 18). The variations of the approximation errors versus Δt in log-scale, are reported in figure 19.

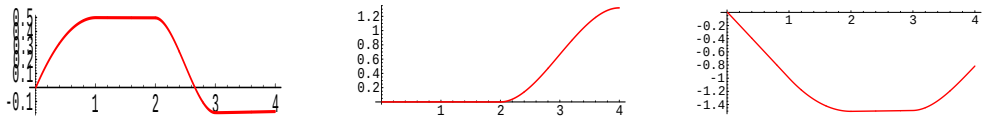

Figure 16. Test prob. 5: (left) the computed $x_1(t)$; (middle) the computed $x_2(t)$; (right) the computed $x_3(t)$

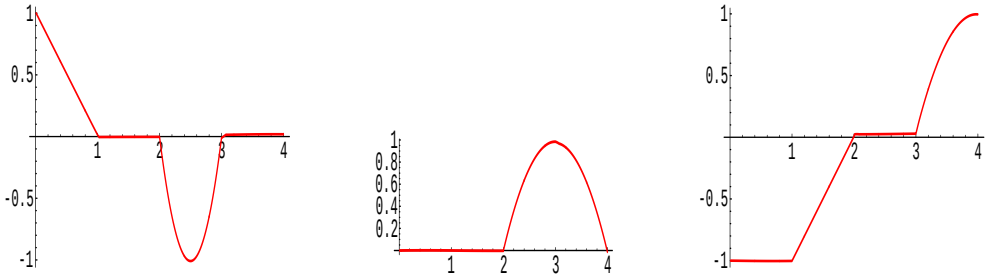

Figure 17. Test prob. 5: (left) the computed $v_1(t)$; (middle) the computed $v_2(t)$; (right) the computed $v_3(t)$

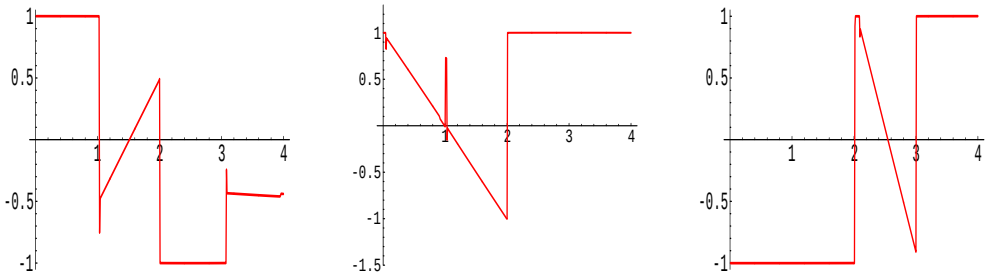

Figure 18. Test prob. 5: (left) the computed $\lambda_1(t)$; (middle) the computed $\lambda_2(t)$; (right) the computed $\lambda_3(t)$

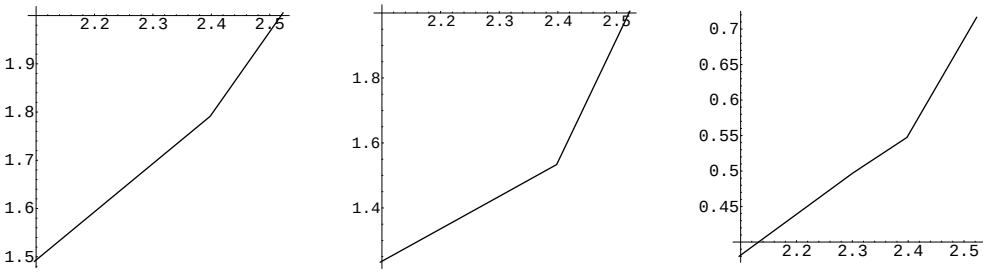

Figure 19. Test prob. 5: (left) L^2-error on $\dot{X}$ versus τ in log-scale; (middle) L^2-error on $\dot{V}$ versus τ in log-scale; (right) L^2-error on λ versus τ in log-scale

Acknowledgments

This work was supported in part by The Institute for Space Systems Operations (ISSO) of the Houston Partnership for Space Exploration and NSF Grant DMS-0244529.

[1] E.J. Dean, R. Glowinski, Y.M. Kuo, G. Nasser, Multiplier techniques for some dynamical system with dry friction, *C.R. Acad. Sc., Paris*, T. 314, Série I, (1992), 153-159.

[2] E.J. Dean, R. Glowinski, Y.M. Kuo, G. Nasser, On the discretization of some second order in time differential equations. Applications to nonlinear wave problems, in *Computational Techniques in Identification and Control of Flexible Flight Structures*, A.V. Balakrisknan ed., Optimization Software, Inc., Los Angeles, (1990), 199-246.

[3] G. Duvaut, J.-L. Lions, Inequalities in Mechanics and Physics, *Springer-Verlag*, Berlin, 1976.

[4] G. Strang, On the construction and comparison of difference schemes, *SIAM J. Num. Anal.*, 5 (1968), 506-517.

[5] R. Glowinski, Numerical Methods for Nonlinear Variational Problems, *Springer-Verlag*, New York, 1984.

[6] R. Glowinski, A. Kearsley, On the simulation and control of some friction constrained motions, *SIAM Journal on Optimization*, Vol 5, No. 3 (1995), 681–694.

[7] H. Cabannes, Study of a vibrating string subject to solid friction, *Math. Methods Appl. Sci.*, 3 (1981), 287-300.

[8] A. Bamberger, H. Cabannes, Mouvement d'une corde vibrante soumise à un frottement solide, C.R., *Acad. Sci. Paris*, 292, I (1981) 269-273.

[9] F. Altpeter, F. Ghorbel, R. Longchamp, Relationship Between Two Friction Models: A Singular Perturbation Approach, *IEEE 37th Conference on Decision and Control*, December 16-18, 1998.

[10] F. Altpeter, F. Ghorbel, R. Longchamp, A Singular Perturbation Analysis of Two Friction Models with Application to a Vertical EDM-Axis, *Proc. IFAC Workshop on Motion Control*,Sept 21-23, 1998, pp. 7-12.

[11] K. Atkinson, W. Han, Theoretical Numerical Analysis, *Springer-Verlag*, New York, 2001.

[12] R. Glowinski, Finite Element Methods for Incompressible Viscous Flow, in Handbook of Numerical Analysis, IX, P.G. Ciarlet and J.L. Lions, eds., North-Holland, Amsterdam, 2003, pp.3-1176.

[13] B. Dacorogna, R. Glowinski, Y. Kuznetsov, T.W. Pan, On a Conjugate Gradient/Newton/Penalty Method for the Solution of Obstacle Problem. Application to the Solution of an Eikonal System with Dirichlet Boundary Conditions. In "Conjugate Gradient Algorithms and Finite Element Methods", M. Křížek, P. Neittaanmäki, R. Glowinski, S. Korotov (Eds.), *Springer*, Berlin, 2004, pp263-283.

[14] R. Glowinski, Y. Kuznetsov, T.W. Pan, On a penalty/Newton/conjugate gradient method for the solution of obstacle problems, *C.R. Acad. Sci. Paris, Série I*, 336(5), 2003, pp.435-440.

[15] R. Glowinski and P. Le Tallec, Augmented Lagrangian and Operator-Splitting Methods in Nonlinear Mechanics, *SIAM Studies in Applied Mathematics*, vol. 9, SIAM, Pennsylvania, 1989.

[16] R. Glowinski, J.L. Lions, R. Trémolières, Numerical Analysis of Variational Inequalities, North-Holland, Amsterdam, 1981.

[17] J.E. Dennis and R.B. Schnabel, Numerical Methods for Unconstrained Optimization and Nonlinear Equation, *SIAM*, Philadelphia, PA, 1996.

[18] N. Kikuchi, J. Oden, Contact problems in elasticity: a study of variational inequalities and finite element methods, *SIAM*, Philadelphia, 1988.

[19] S. Cull,R. Tucker, On the modelling of Coulomb friction, *J. Phys. A: Math. Gen.*, vol. 32, pp. 2103-2113, 1999.